Research Paper

Assessment of Polymeric Nanoparticles to Enhance Oral Bioavailability and Antioxidant Activity of Resveratrol

R. HASIJA[1], S. CHAURASIA[2] AND SWATI GUPTA*

Department of Pharmaceutics, Amity Institute of Pharmacy, Amity University, Noida, Uttar Pradesh 201301, [1]Formulation Research and Development, Mankind Research Centre, Gurgaon, Haryana 122050, [2]Innovation and Pharma Research and Development, Ashland Specialty Ingredients, Hyderabad, Telangana 500078, India

Resveratrol has proven as potential natural antioxidant, non-flavonoid polyphenolic compound, but it has limitations such as low water solubility, which substantially restricts oral bioavailability. To enhance oral bioavailability and antioxidant potential of resveratrol by fabricating the resveratrol encapsulated oral eudragit® E100 based polymeric nano-delivery system. Resveratrol-encapsulated polymeric nanoparticles were developed by solvent extraction and diffusion method. Copolymer, eudragit® E100 polymeric matrices were used to prepared polymeric nanoparticles and *in vitro* physicochemically characterized. Furthermore, *in vivo* pharmacokinetic and antioxidant potential of optimized resveratrol-encapsulated polymeric nanoparticles was evaluated. The resveratrol-encapsulated polymeric nanoparticles exhibited optimum mean particle size (410±9.78 nm), polydispersity index (0.203±0.079) and encapsulation efficiency (66.88±5.45 %), respectively. *In vitro* release profile of resveratrol showed >25 % release in first 2 h in phosphate-buffered saline pH 7.4 followed by >75 % at the end of 48 h. The optimized resveratrol-encapsulated polymeric nanoparticles were stable at the accelerated condition and room temperature, respectively. The optimized resveratrol-encapsulated polymeric nanoparticles demonstrated significantly higher oral bioavailability (~4.07-fold; $p<0.05$) as compared to pure resveratrol. Furthermore, the optimized resveratrol-encapsulated polymeric nanoparticles were evaluated for free radical scavenging activity and showed to increase the activity with time i.e. after 72 h, it was the same as pure resveratrol but at 24 h no increase in antioxidant activity was observed with optimized resveratrol-encapsulated polymeric nanoparticles. Furthermore, half-maximal inhibitory concentration of the optimized resveratrol-encapsulated polymeric nanoparticles was decreased with time. Results are suggesting that resveratrol-encapsulated polymeric nanoparticles are the promising approach using eudragit® E100 as a polymeric material to enhance oral bioavailability and antioxidant potential of insoluble resveratrol.

Key words: Resveratrol, eudragit® E100, oral polymeric nanoparticles, bioavailability, antioxidant activity

The oxygen metabolism produces exogenous factors or by-products, which repeatedly produce the Reactive Oxygen Species (ROS) inside the human body[1]. However, high concentrations of ROS, oxidative stress can stimulate damage of Deoxyribonucleic Acid (DNA), activate cancer cells, degeneration, vascular and other diseases[2]. Many antioxidants are shown promising additional beneficial cellular effects through modulation processes at specific biochemical levels such as protein synthesis and signaling pathways[3]. Therefore, to neutralize high production of ROS and reduce oxidative stress by externally supplied enzymes, antioxidant and endogenous factors are used such as superoxide dismutase, catalase and glutathione peroxide[4]. However, the novel antioxidant is being screened from natural and synthetic sources[5].

The use of exogenous antioxidant, mainly naturally derived compounds have acknowledged an enormous interest in the modern era for their prophylactic and therapeutic potential against ROS is compromised. The natural, non-flavonoid polyphenolic compound i.e. trans-Resveratrol (Res), mainly present in more

Accepted 06 November 2021
Revised 19 July 2021
Received 01 December 2020
Indian J Pharm Sci 2021;83(6):1114-1128

***Address for correspondence**
E-mail: sgupta24@amity.edu

than 70 plant species, including human foods such as grapes, peanuts, Japanese knotweed, Itadori tea, soy and red fruits[6-8] is used. Many studies have been demonstrated that Res shows numerous desirable biological activities including high antioxidant activity[9], anti-inflammatory, cardioprotection, anti-platelet aggregation, vasodilation, antiviral activity, prolongation of lifespan, neurodegenerative diseases, estrogenic functions and cancer chemoprotective activity[10-14]. Apart from the numerous therapeutic activity in several experimental models, the clinical applications of Res have been restricted because of its low water solubility (~3 mg/100 ml) and log P~3.1[15]. Despite the poor water solubility of Res, its membrane permeability is quite high and can come under class II compound in the biopharmaceutical classification system[16]. Therefore, beneficial application of Res remains very restricted due to its short biological half-life, labile properties, quick metabolism and elimination[17] indicate that the deprived bioavailability (approximately <1.0 %, when orally administered), thereby limit the use of Res in therapeutic systems[18]. After oral administration of Res, the plasma half-life was found to be only 15 min[19,20]. Moreover, Res is a polyphenolic compound containing hydroxyl groups (3, 5, 40-positions of the stilbene moiety) which is suitable substrates for conjugation reactions i.e. glucuronidation and sulfation thereby Res extensively metabolized in phase II[21-23]. Although several strategies have been adopted to rectify the troubles interrelated with a half-life, *in vitro* release, intensive metabolism and bioavailability problems of Res such as solid lipid nanoparticles, biodegradable Polymeric Nanoparticles (PNPs), liposomes, micro and nanoemulsions technique is used[21]. Apart from these strategies recently few more techniques are also involved to increase the bioavailability of Res which includes, amorphous solid dispersions of eudragit E/Hydrochloric Acid (HCl)[24] using spray drying approach, microspheres of eudragit® retard polymer[25], Gamma (γ) cyclodextrin inclusion complexes[26] and Hydroxypropyl-Beta (HP-β) cyclodextrin or β-cyclodextrin inclusion complexes[27]. But the problems associated with these strategies are complex processes, Drug Loading (DL) issues, sometimes stability problems, cost-effective and non-uniformity of the drug:polymer blending process.

In this context, the PNPs are an excellent approach and colloidal carriers for poorly water-soluble antioxidant to conflict these above disadvantages. The process variables along with *in vitro* physicochemical studies of PNPs influence the *in vivo* pharmacokinetic parameters as well as antioxidant properties of the Res. Furthermore, PNPs demonstrated a prolonged and sustained release profile of Res which supports to diminishes the toxicity[28]. In PNPs preparations, Eudragit® E100 (EE100) copolymer was used to prepare Res encapsulated PNPs and act as colloidal carriers. EE100 copolymer is the 1:2:1 ratio of methyl methacrylate, N,N-dimethylaminoethyl methacrylate and butyl methacrylate monomers has been usually incorporated to increase the solubility of poorly water-soluble antioxidant compound which can be oppressed in many drug delivery systems[29]. Particle Size (PS), Zeta Potential (ZP) values and composition of PNPs take part in encapsulation and enhanced the scavenging activity of Res in PNPs[9]. Thus, to the best of our knowledge, there is no scientific literature reflect to develop this novel PNPs system to enhance the oral bioavailability and antioxidant potential of the water-insoluble drug, Res.

Therefore, the principle purpose to achieve high dissolution and oral bioavailability profile, better antioxidant potential and no side effects of Res, oral PNPs is extremely advantageous strategies. The present investigation suggested that the emulsification-diffusion-evaporation technique was employed to prepare Res-Encapsulated Polymeric Nanoparticles (Res-PNPs). "Taguchi orthogonal array design" was used to check the effect of independent variables on dependent response variables i.e. mean PS and Encapsulation Efficiency (EE). The optimized Res-PNPs were analyzed for the physical state as well as *in vitro* physicochemical studies. The *in vitro* release study of optimized Res-PNPs was performed up to 48 h. The stability study of optimized Res-PNPs was performed in real-time (25°±2°/60 %±5 % Relative Humidity (RH)) for 9 mo as well as at accelerated condition (40°±2°/75 %±5 % RH) for 6 mo. Further, *in vivo* pharmacokinetic parameters of the optimized Res-PNPs were performed in healthy Charles Foster rats. Furthermore, the optimized Res-PNPs were analyzed to check their ability to scavenge the radical, 2,2'-Azino-bis(3-ethylbenzthiazoline-6-sulfonic acid) diammonium salt ($ABTS^{\cdot+}$).

MATERIALS AND METHODS

Materials:

Res was provided by Cayman Chemical Company, USA. EE100 and Poloxamer 188 (PLX188) were gifted from Evonik Degussa, Mumbai and Mankind Pharma Ltd., Okhla, India. Chloroform, ethanol and methanol were purchased from SD Fine-Chem Ltd (Mumbai,

India). Nanofree™ grade water (Barnstead, Dubuque, IA) was used for all the studies. ABTS and potassium persulfate were obtained from Sigma-Aldrich, USA. All other chemicals used in this study were of analytical grade.

Preparation of Physical Mixture (PM):

The PM of Res, EE100 and PLX188 was prepared manually using pestle and mortar in a mass ratio of 0.027:4.7:0.85 g. The mixing time was 10 min followed by sieved through #40 to obtain a homogeneous mixture and stored in a desiccator till further use.

Preparation of Res-PNPs:

The emulsification-diffusion-evaporation technique was employed to prepared Res-PNPs with the small modification[30]. The independent variables such as drug-polymer ratio, amount of ethyl acetate, homogenization speed and PLX188 concentration were used to prepare Res-PNPs. Briefly, Res and EE100 were dissolved in the organic solvent, ethyl acetate and stirred using a magnetic stirrer (IKA®, C-MAG, HS7, Germany) for 10 min. Then, the prepared organic solution was consequently added drop by drop to 50 ml aqueous PLX188 solution using a syringe at a distance of ~4 cm above the surface of the external aqueous phase under homogenizer (Dhian Scientific, M30, South Korea) for 10 min. Thereafter, 25 ml of water was added into the final emulsion to allow diffusion of the organic solvent into the water followed by magnetically stirring at room temperature for 24 h to evaporate the organic solvent and formation of Res-PNPs. Further, the prepared Res-PNPs were centrifuged (Refrigerated Centrifuge (RC) 4100 F, Eltech, Mumbai, India) at 15 000 rpm for 30 min. The prepared sediment was washed with water and resuspended in water containing 2 % w/v mannitol as a cryoprotectant and lyophilized using lyophilizer (Freezone, Labconco, USA). Finally, the lyophilized Res-PNPs were stored in glass vessels till further use.

PS, Polydispersity Index (PDI) and ZP:

The PS and ZP of Res-PNPs in dispersion were determined using the Delsa™ Nano C particle size analyzer (Beckman Coulter, Inc., USA). For PS measurement, dispersions were dispersed in distilled water and put into cuvettes of PS analyzer and measured the PS and PDI of the PNPs. The mean PS was determined from triplicate measurements of each sample. Similarly, samples were placed in a zeta cell and the ZP was measured.

EE and DL:

EE and DL of Res-PNPs were evaluated by a direct method after 24 h of preparation using High-Performance Liquid Chromatography (HPLC). Briefly, 10 mg of Res-PNPs was dissolved in 1 ml of methanol followed by dilution with the mobile phase. The diluted PNPs solution was filtered through a 0.45 µm syringe filter (Polyethersulfone (PES) grade, Millipore, Bedford, USA) and injected into the HPLC system for quantification at a wavelength of 306 nm. The Percentage (%) EE and % DL of Res-PNPs were calculated according to the following equations:

% EE=(Amount of Res encapsulated/Total amount of Res used)×100

% DL=(Amount of Res loaded/Total amount of the prepared formulations)×100

Taguchi L_9 orthogonal array design:

A Taguchi L_9 (3^4) orthogonal array design factors (independent and dependent) and Analysis of Variance (ANOVA) statistical analysis were adopted by using MINITAB® 17 software to decide the optimal conditions related to selected independent factors which should be used to establish an optimized formulation composition of Res-PNPs with minimal PS and high % EE. The L_9, 3-level 4-factors experimental design such as drug:polymer ratio, the amount of ethyl acetate, homogenization speed and PLX188 concentrations. The four independent variables each at three levels (low, medium and high) would give only nine experimental trials as depicted in Table 1. Also, robustness, suitability and reliability of Taguchi orthogonal array design were determined to be prepared and characterizing Res-PNPs formulation at an optimized level of independent factors and their dependent responses. The experiments were performed thrice and characterized various parameters[31,32].

Compatibility studies of Res-PNPs:

Fourier-Transform Infrared (FT-IR) spectroscopy studies: The FT-IR spectra of pure Res, EE100, PM and optimized Res-PNPs were evaluated by FT-IR spectrophotometer (Shimadzu, 8400S, Tokyo, Japan) to monitor any significant change if occurs, between Res and components of Res-PNPs, both after and before the encapsulation of Res. The small quantity of each component was triturated gently with anhydrous Potassium Bromide (KBr) and compressed to form a thin pellet in the FT-IR sample holder. The scanning

TABLE 1: TAGUCHI ORTHROGONAL ARRAY DESIGN OF EXPERIMENT AND CORRESPONDING PHYSICOCHEMICAL CHARACTERIZATIONS OF DIFFERENT RES-PNPs BATCHES (ALL VALUES ARE REPORTED IN MEAN±SD; n=3)

Batches	A	B	C	D	PS (nm)	ZP (mV)	PDI	% EE	% DL
Res-ENP1	01:04	2.5	8000	0.5	599±1.35	10.2±1.17	0.513±0.071	63.45±3.93	0.886±0.082
Res-ENP2	01:04	5	10000	1	502±5.41	19.2±1.73	0.411±0.052	61.38±4.12	0.627±0.047
Res-ENP3	01:04	7.5	12000	1.5	410±9.78	38.1±2.56	0.203±0.079	66.88±5.45	0.512±0.065
Res-ENP4	01:06	2.5	10000	1.5	762±6.06	24.7±3.71	0.401±0.056	67.65±7.29	1.134±0.017
Res-ENP5	01:06	5	12000	0.5	645±6.94	17.3±6.26	0.487±0.058	75.66±1.92	0.617±0.049
Res-ENP6	01:06	7.5	8000	1	687±9.87	15.3±1.98	0.472±0.057	70.98±5.16	0.413±0.013
Res-ENP7	01:08	2.5	12000	1	578±9.27	23.8±6.35	0.341±0.089	52.47±2.19	1.244±0.046
Res-ENP8	01:08	5	8000	1.5	745±1.94	28.6±7.42	0.397±0.052	69.37±6.49	0.703±0.021
Res-ENP9	01:08	7.5	10000	0.5	619±7.47	19.7±1.64	0.822±0.055	65.22±3.22	0.412±0.011

Note: Where, A-Drug:polymer ratio; B-Amount of ethyl acetate (ml); C-Homogenization speed (rpm); D-PLX188 concentration (% w/v); PS-Mean particle size; ZP-Zeta potential; PDI-Polydispersity index; % EE-Percent entrapment efficiency; % DL-Percent drug loading

was performed over the wavenumber ranging from 4000-400 cm^{-1} at room temperature and resolution was set at 4 cm^{-1}.

Differential Scanning Calorimetry (DSC): The physical state of Res inside PNPs and compatibility of Res with each component of PNPs were evaluated by DSC. The thermograms were recorded using DSC Q1000 (TA Instruments, USA) which was previously calibrated with indium. The weighed samples (2 mg) were sealed in aluminum pans and scanned at a heating rate of 10° min^{-1} over the temperature range of 30-275°, under a nitrogen atmosphere with a flow rate of 50 ml min^{-1}.

X-Ray Diffraction Analysis (XRD): X-ray diffraction patterns of pure Res, EE100, PM and optimized Res-PNPs were examined using XRD (Bruker D8 Discover) with Nickel (Ni) filtered Copper K Alpha-1 (Cu-$K\alpha_1$) radiation at 45 kV and 40 mA. The scattered radiation in crystalline regions of samples was measured with a vertical goniometer. The diffraction patterns were obtained between 10° and 50° angle using a step size of 0.045° with a detector resolution in 2θ at 25°.

Transmission Electron Microscopy (TEM) study: The structure and shape of the optimized Res-PNPs were examined by employing High-Resolution Transmission Electron Microscopy (HR-TEM). In short, a drop of appropriately diluted Res-PNPs was placed on the carbon-coated copper grid. After 1 min of adsorption, excess liquid was wicked off with filter paper and air-dried at room temperature. Then, the grid was examined using HR-TEM (TECHNAI 20G2, FEI Company, Netherlands, Holland) at an accelerating voltage of 200 kV with different magnifications. Moreover, the electron diffraction pattern of optimized Res-PNPs revealed the amorphous diffraction halo inside the matrix of PNPs along with the absence of star shape particles.

Atomic Force Microscopy (AFM) study: The morphology of optimized Res-PNPs was inspected by mounting on AFM scanner (NT-MDT, Moscow, RUSSIA) using Solver next software. A drop of PNPs dispersions (1 mg/ml) was placed on freshly cleaved mica. Then, after 5 min of incubation, the surface was gently rinsed with deionized water to remove unbound optimized Res-PNPs. The sample was air-dried at room temperature and mounted on the microscope scanner and captured in noncontact mode with a scanning rate of 0.5 Hz.

***In vitro* release study:** *In vitro* release of pure Res and optimized Res-PNPs were evaluated using dialysis membrane technique with a cutoff molecular weight of 12 000-14 000 Da. Dialysis bag filled with phosphate buffer, pH 7.4 containing 0.1 % w/v of Tween 80[33] and optimized Res-PNPs equivalent to 2 mg of Res and placed in 50 ml of release medium stirring at 100 rpm at 37° using a magnetic stirrer. Aliquots (1 ml) were picked off at predetermined time intervals (0, 0.5, 1, 2, 3, 4, 5, 6, 8, 12, 24 and 48 h) and replace with an equal volume of the same fresh medium to maintain sink condition. The quantification of aliquots sample was examined using HPLC at 306 nm wavelength. Further, the zero-order, first-order, Higuchi and Korsmeyer-Peppas model was applied to evaluate the drug release kinetics and mechanism.

Stability study of Res-PNPs: Stability studies were performed to assess the storage stability of optimized Res-PNPs at room temperature (25±2°, 60±5 % RH) for 9 mo and at accelerated conditions (40±2°, 75±5 % RH) for 6 mo to check any changes in physicochemical properties such as mean PS, PDI and % EE.

***In vivo* pharmacokinetic study:**

Animals and dosing: The Central Animal Ethical Committee (Committee for the Purpose of Control and Supervision of Experiments on Animals (CPCSEA)) approved the protocol for pharmacokinetic study. Healthy Charles Foster rats of either sex (weighed, 150-200 g) were housed in polypropylene cages over dust-free husk for 1 w before the day of experiments with 12 h light/dark cycle at 25±2° and 40-70 % RH. The rats were fed with chow and water *ad libitum*[34]. The animals were divided into three groups, Group I (n=6) and Group II (n=6) which received pure Res and PM (solubilized in 0.3 % sodium carboxymethylcellulose in purified water), respectively and Group III (n=6) received optimized Res-PNPs (equivalent to 25 mg/kg of Res) were given oral route using needle gavages. Blood samples (200 µl) were withdrawn via retro-orbital plexus with predetermined time points (0, 0.25, 0.5, 0.75, 1, 2, 4, 8, 12 and 24 h) and collected in heparinized Eppendorf tubes. Further, plasma was separated out instantaneously centrifugation at 5000 rpm for 10 min at -4° and stored at -20° until further analysis.

Chromatography setting and extraction techniques:

The quantification of Res was assessed by Reverse-Phase (RP)-HPLC as scientifically reported earlier[35]. The HPLC system consists of inline degasser, 515 HPLC binary pump (Waters, USA), rheodyne 7752i manual injector (Waters, USA), C_{18} reverse-phase (250×4.6 mm, 5 µm) Octadecyl-Silica 2 (ODS-2) column protected with a guard column (12×4.6 mm, 5 µm) (Waters, USA) and a photodiode array detector (Waters, USA). The mobile phase methanol:phosphate buffer, pH 6.8 (pH adjusted with 0.5 % v/v orthophosphoric acid solution in Milli-Q water) with the ratio of 63:37 % v/v along with the flow rate was set at 1.0 ml/min. The column temperature was maintained at 25±2° using a column oven (Waters, USA) and effluent was detected at 306 nm. Peak area and retention time were determined by operating software Empower Node 2054. Calibration curves were drawn in the range of 10-5000 ng/ml. The run time was found to be 6.4 min at a temperature of 25°. The actual Res concentration in plasma samples was estimated from the calibration curve prepared by spiking the known concentration of Res in plasma and analyzed using RP-HPLC.

A liquid-liquid extraction procedure was adopted for the separation of Res from the plasma[36]. Plasma with Res and internal standard (Caffeine, 0.436 mg/ml) was thawed, 100 µl was transferred to 1.5 ml Eppendorf tube and 900 µl of mobile phase was added to precipitate plasma proteins. This spiking mixture was vortexed for 5 min and centrifuged at 5000 rpm for 10 min. The supernatant was transferred to a glass tube and evaporated in a vacuum oven at 40°. The dried residue was reconstituted with 100 µl mobile phase and 20 µl of samples was filtered through a 0.2 µm syringe filter (PES grade, Millipore, Bedford, USA) and injected into RP-HPLC column for quantification of Res[37].

Antioxidant activity:

The antioxidant activity of pure Res, PM and optimized Res-PNPs were assessed using cation radical $ABTS^+$. A combination of $ABTS^+$ (7 mM) and potassium persulfate (2.45 mM) was primed and permitted to be kept at room temperature[38,39]. The $ABTS^+$ solution was diluted with 50 mM phosphate buffer, pH 7.4 at an absorbance of 734 nm. For the antioxidant effects of pure Res, PM and optimized Res-PNPs, a different range of concentrations from 1 to 25 µM was used. The prepared compounds were incubated at 37° under continuous agitation and confined from light at 0, 24, 48 and 72 h. After incubation at 37°, aliquots with desired concentrations were incubated for 30 min with $ABTS^+$ and absorbance was assessed at 734 nm. The phosphate buffer solution was used as a control for this study.

The percentage of inhibition was calculated by the following equation:

$$\text{Percentage inhibition}=(A_c-A_t/A_c)\times 100$$

Where A_c is the absorbance of control and A_t is the absorbance of the test.

The inhibitory concentration of $ABTS^+$ at 50 % i.e., Half-Maximal Inhibitory Concentration (IC_{50}) was calculated by the linear regression of Res concentration versus percentage of $ABTS^{-+}$ inhibition curves.

Statistical evaluation:

The statistical evaluation (ANOVA) was computed using Graph pad prism software (version 5.03). All the experiments were performed in triplicate and results were expressed as mean±Standard Deviation (SD) for *in vitro* studies and mean±Standard Error of the Mean (SEM) for *in vivo* studies.

RESULTS AND DISCUSSION

Results of the PS of different Res-PNPs batches were found to be in the range of 410.42±9.78 nm (Batch Res-ENP3) to 687.12±9.87 nm (Batch Res-ENP6) as

shown in Table 1. The drug:polymer (concentration of the drug is constant) ratio plays an important role to influence the PS of Res-PNPs. Therefore, raise in the drug:polymer ratio accelerates the construction of bigger size droplet most likely due to enhanced organic phase (ethyl acetate) viscosity, which in due course leads to mired dispersion of organic phase in the aqueous phase which follow-on to enhanced PS after removal of organic phase[40]. Further, increased concentration of PLX188 resulted in smaller PS because PLX188 develops boundary layer around PNPs droplets, which prevents impingement of droplets and subsequently formation of non-aggregated polymeric dispersion[41]. Furthermore, an increased amount of ethyl acetate resulted in decreased mean PS due to reduced viscosity of organic phase followed by maximum dilution of polymer. Moreover, increased homogenization speed provides shear force to decrease mean PS and vice-versa.

PDI values of different Res-PNPs batches were found to be ranging from 0.203±0.079 (Batch Res-ENP3) to 0.472±0.067 (Batch Res-ENP6) as presented in Table 1. PDI values determine the level of homogeneity (PDI<0.25) and heterogeneity (PDI>0.3) of the PNPs. The batch with Res-ENP3 showed a smaller PDI value indicates stable and homogeneous dispersion of PNPs, whereas the batch with Res-ENP6 showed a higher PDI value which favors the destabilization of PNPs due to Ostwald ripening[42]. ZP is the main constraint for determining the physical stability of PNPs. Its high value demonstrated that stable colloidal dispersion followed by PNPs non-aggregation due to repulsion forces between PNPs. The positive or negative ZP values of the PNPs were revealed by electrophoretic mobility measurements. Thus, the prepared Res-PNPs exhibited positive ZP values due to the presence of polymer terminal carboxylic groups. The ZP values of prepared Res-PNPs were found to be ranging from +38.1±2.56 (Batch Res-ENP3) to +10.2±1.17 mV (Batch Res-ENP1) as presented in Table 1 which demonstrated a high electric charge onto the surface of PNPs which resulted in that more stable formulation[43].

Results of the % EE and % DL of different batches of Res-PNPs formulations are shown in Table 1. Many independent variables such as drug:polymer ratio, organic phase (internal phase) and aqueous phase (external phase) were tailored to accomplish desirable % EE and % DL of Res-PNPs. During the entrapment process, an aqueous PLX188 solution was used as an external phase to hamper the degradation of Res. The % EE values were found to be ranging from 52.47±2.19 % (Batch Res-ENP7) to 75.66±1.92 % (Batch Res-ENP5) whereas, % DL values ranging from 0.412±0.011 % (Batch Res-ENP9) to 1.244±0.046 % (Batch Res-ENP7) which attributed to excellent drug:polymer affinity[44]. At excellent drug:polymer ratio, the viscosity of organic phase (ethyl acetate) enhances which eventually decreases the net shear stress at the time of emulsification which resulted in larger PNPs droplets followed by decreased drug diffusion into external PLX188 phase as resulted that high entrapment of Res. In contrast, a high level of organic-aqueous affinity leads to enhanced stress and interfacial tension of emulsion droplets which resulted in the development of the bigger size of emulsion droplets during the emulsification process which is harsh for organic phase diffusion to external PLX188 solution[45], resulted that excellent % EE and % DL. The % EE and % DL depends on the Res solubility in the excipients matrix materials (solid polymer or liquid dispersion agent), which is correlated to matrix composition, molecular weight, drug-polymer interactions and presence of functional end groups in either the drug or matrix[46-48]. Res comes under small molecules which indicates the use of ionic interaction between drug and polymer matrix materials can be very effective in enhancing % EE and % DL[49,50].

Taguchi orthogonal array design qualitatively analyzes the correlations between independent variables at diverse levels by scheming an orthogonal table and drawing statistical analysis based on the various process parameters. A Taguchi orthogonal array design at four independent variables and three levels were applied and optimize the best formulation composition[51]. The dependent variables considered were mean PS and % EE. The range of mean PS and % EE was found to be 410±9.78 to 762±6.06 nm and 52.47±2.19 to 75.66 ±1.92 %, respectively. However, based on the results of mean PS and % EE, it was very difficult to select the optimized formulation composition. Therefore, the mean value of PS (PS_i), mean value of EE (EE_i), delta values and corresponding rank of each response that influenced the mean PS are listed in decreasing order as follows C>D>B>A. Moreover, the factor's influences on mean PS at individual levels within each factor are explained by PS_i and can be ranked as A: 1>2>3; B: 2>1>3; C: 3>1>2; D: 3>2>1. So, the resultant optimum formulation composition should be $A_1B_2C_3D_3$. Similarly, the factors influencing % EE was in the order of B>A>C>D based on the delta value and the individual levels within each factor are ranked as A: 1>2>3; B: 3>1>2; C: 1>3>2; D: 3>1>2 as shown in Table 2. The

highest % EE could be observed at $A_1B_3C_1D_3$, which showed that both responses cannot have their preferred values at the same variable setting. ANOVA results along with delta value recommended that factors C and D were highly significant for mean PS which is having p value of 0.012 and 0.005, respectively at a 95 % confidence interval. Thus, the other two factors can be arbitrarily affecting the response. The p values of factors A and B were found to be 0.007 and 0.005, respectively at a 95 % confidence interval for the highest % EE as presented in Table 3. Thus, the level setting C_3D_3 and A_1B_3 were significant factors for mean PS and % EE, respectively. Therefore, mean PS and % EE was considered to be reasonably the most important response parameters and the established optimized formulation compositions were found to be 1:4 (w/w) Res/EE100 ratio, 7.5 ml ethyl acetate, 12 000 rpm homogenization speed and 1.5 % w/v PLX188 concentration i.e. batch Res-ENP3.

Results of the FT-IR spectra of pure Res EE100, PM and optimized Res-PNPs (batch Res-ENP3), are shown in fig. 1. Pure Res exhibited its characteristics absorption bands at 3088.7 cm^{-1} for O-H stretching of the alcoholic group, 1606.7 cm^{-1} for C-C stretching of the olefinic group, 1442.8 cm^{-1} and 1587.4 cm^{-1} for C=C stretching of the aromatic ring, 1153.4 cm^{-1} for C-O stretching and 964.4 cm^{-1} for trans olefinic bond [fig. 1(a)][52]. Further, FT-IR spectra of EE100 [fig. 1(b)] demonstrates characteristics absorption bands at 2858 cm^{-1}, which indicate the presence of -CH_2 symmetric stretching, at 1728 cm^{-1} indicates C=O carbonyl stretching[31].

TABLE 2: EXPERIMENTAL SIGNAL TO NOISE (S/N) RATIO FOR THE RESPONSE PARAMETERS AT DIFFERENT LEVELS OF PREPARED RES-PNPs ACCORDING TO TAGUCHI ORTHOGONAL ARRAY DESIGN

Levels	Independent factors			
	A	B	C	D
PS_1	-54.89	-54.84	-55.13	-55.46
PS_2	-54.99	-55.78	-53.37	-54.17
PS_3	-54.98	-54.73	-56.22	-56.11
Delta value	0.10	1.05	2.85	1.94
Rank	4	3	1	2
EE_1	-13.45	-11.12	-11.46	-12.01
EE_2	-11.93	-10.08	-12.75	-11.67
EE_3	-10.65	-13.61	-12.23	-12.27
Delta value	2.8	3.53	1.29	0.6
Rank	2	1	3	4

Note: PS_i and EE_i is the mean value of PS and EE. Delta value is the difference between the maximum value and the minimum value of PS_i and EE_i

TABLE 3: ANOVA TABLE FOR THE RESPONSE PARAMETERS OF PS AND EE

Factors	DoF	SS	MS	% PC	F[a]	P[b]
PS						
A	(2)	(14.8245)	(7.4123)	58.2925	Pooled	
B	(2)	(1.2359)	(0.6179)	4.8597	Pooled	
C	2	9.2459	4.6229	36.3565	1.151	0.012
D	2	0.1249	0.0625	0.4911	0.015	0.005
Pooled error	(4)	(16.0604)	(4.0151)			
SS_{Total}	8	25.4312		100		
% EE						
A	2	1.4378	0.7189	1.8747	0.043	0.007
B	2	7.6892	3.8446	10.0260	0.227	0.005
C	(2)	(14.2196)	(7.1098)	18.5410	Pooled	
D	(2)	(53.3459)	(26.6729)	69.5581	Pooled	
Pooled error	(4)	(67.5655)	(16.8913)			
SS_{Total}	8	76.6925		100		

Note: DoF-Degree of freedom; SS-Sum of squares; MS-Mean of squares; % PC-Percent contribution; F-Fisher test [a]$F<0.05$ (2, 4)=6.94; [b]$p<0.05$, Significant in C and D for PS and in A and B for % EE

Therefore, all major peaks of Res and EE100 were observed in FT-IR spectra of PM, as illustrated in fig. 1(c). The optimized Res-PNPs exhibited all the characteristics of absorption peaks of Res with minor shifts in absorption bands as depicted in fig. 1(d). In optimized Res-PNPs, the peak at 3,088 cm^{-1} becomes wider which exhibits hydrogen bonding in increased or enhanced. The C-C stretching of the olefinic group at 1635.6 cm^{-1}, C=C stretching of the aromatic ring at 1464.02 cm^{-1}, C-O stretching at 1147.68 cm^{-1} and trans olefinic band at 966.37 cm^{-1} was observed. The existence of all characteristics absorption bands of Res in the optimized Res-PNPs proved that there is the absence of chemical interaction between Res and other formulation excipients.

Results of the DSC thermograms of pure Res, EE100, PM and optimized Res-PNPs are shown in fig. 2. Pure Res exhibited a melting temperature of Res followed by a sharp endothermic decomposition peak at 267.71°[53]. However, this melting peak was absent in the thermogram of optimized Res-PNPs. It was proved that Res was entrapped inside the PNPs as an amorphous form[54].

Results of the Powder X-ray Diffraction (pXRD) study confirm the absence of drug crystallinity. pXRD analysis of pure Res, EE100, PM and optimized Res-PNPs are shown in fig. 3. Pure Res exhibited crystalline nature and sharp diffraction peaks at 6.62°, 13.2°, 16.36°, 19.18°, 22.28°, 23.54°, 25.18°, 28.26°, 31.6°, 38.32° and 45.18° in 2θ scale as depicted in fig. 3(a)[55]. The EE100 does not exhibit any characteristic peaks at 2θ angles as shown in fig. 3(b). In the case of PM, none of the peaks disappeared which is shown in fig. 3(c). Since EE100 showed the absence of characteristic peak but diffraction peak must be developed from the crystalline form of Res. These results demonstrated that Res was partially present in crystalline form in the PM. Further, the melting of EE100 in PM formulation dissolved some of Res resulted in that partial transformation into an amorphous form. In contrast, optimized Res-PNPs exhibited no other characteristics sharp peaks as depicted in fig. 3(d). The above results recommended the absence of crystallinity and the presence of amorphous nature in the PNPs matrix of Res-ENP3. Additionally, XRD results associated with DSC results proved that the transformation of Res from crystalline state to amorphous form[54].

Results of the HR-TEM micrographs assessed the surface morphology of the optimized Res-PNPs. Fig. 4a depicted the development of spherical, smooth and more or less uniform size distribution followed by a low PDI (Table 1) of optimized Res-PNPs. Further,

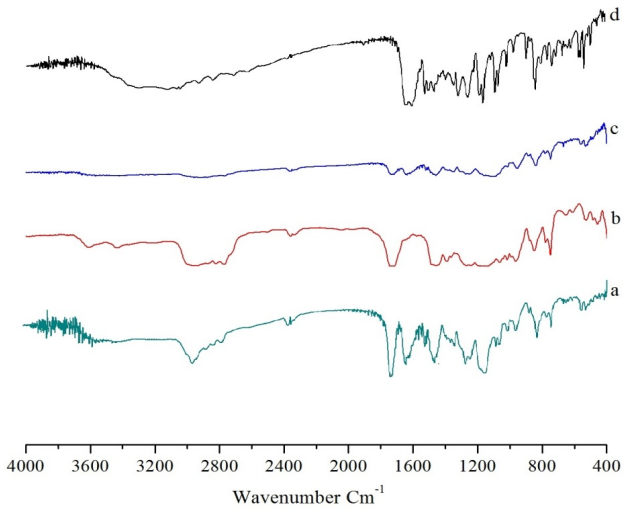

Fig. 1: FT-IR spectra of (a) Pure Res; (b) EE100; (c) PM and (d) Optimized Res-PNPs

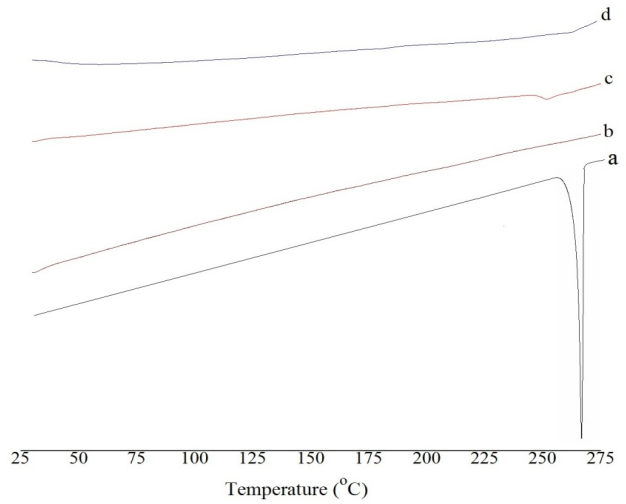

Fig. 2: DSC thermograms of (a) Pure Res; (b) EE100; (c) PM and (d) Optimized Res-PNPs

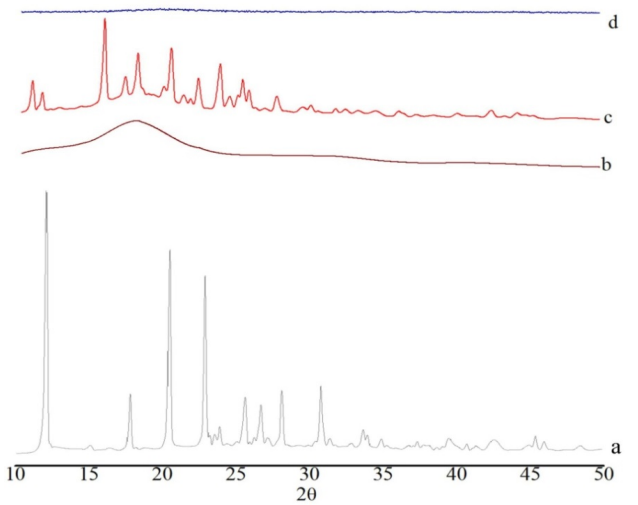

Fig. 3: pXRD curves of (a) Pure Res; (b) EE100; (c) PM and (d) Optimized Res-PNPs

fig. 4b illustrated the electron diffraction of optimized Res-PNPs which revealed the amorphous halo pattern. These micrographs reveal the absence of star-shaped particles in ring patterns and homogeneous drug distribution inside the matrix of PNPs[56,57].

Results of the AFM micrographs exhibited well-separated spherical shapes along with smooth surfaces of optimized Res-PNPs as depicted in fig. 4c (Three Dimensional (3D) image). Further, the micrographs also showed that almost uniform size distribution with a low PDI, which has an average diameter smaller than 410 nm as examined by the PS analyzer as illustrated in fig. 4d.

Results of the *in vitro* release study of pure Res and optimized Res-PNPs in Phosphate-Buffered Saline (PBS, pH 7.4 as depicted in fig. 5. The result recommended that pure Res remained undissolved in PBS, pH 7.4 whereas, optimized Res-PNPs gave >25 % release in the first 2 h followed by >75 % release at the end of 48 h due to the amorphous nature of Res and structural homogeneity in the PNPs matrix which assist higher solubility in PBS. However, the burst effect was showed during the first 30 min (being more than 15 %) because of immediate release of the surface-bound drug then the mechanism of hydration, polymer swelling or polymer erosion takes place which leads to diffusion-based sustained release of the drug. The presence of EE100 polymer along with surfactant (PLX188) leads to smaller PNPs which renders a massive surface area to volume ratio and facilitating greater interaction between PNPs and gut absorption site, which eventually results in a significant enhancement in the absorption of an incorporated drug. Additionally, smaller PNPs not only defend the drug from the gastrointestinal milieu but also evade the first-pass metabolism by lymphatic uptake via Microfold (M) cells of Peyer's patches and thus diminish the dose and related toxicity. The hydration of polymer brings about extension in diffusional path length of drug which subsequently lowers their diffusion rate[58]. Therefore, the relative hydration rate and integrity of the hydrated polymer matrix is the prime mechanism that maintains and facilitates the sustained release profile of PNPs. Thus, the above results suggested that the sustained release of PNPs was governed by the amalgamation of drug diffusion and polymer chain relaxation during polymer swelling[59].

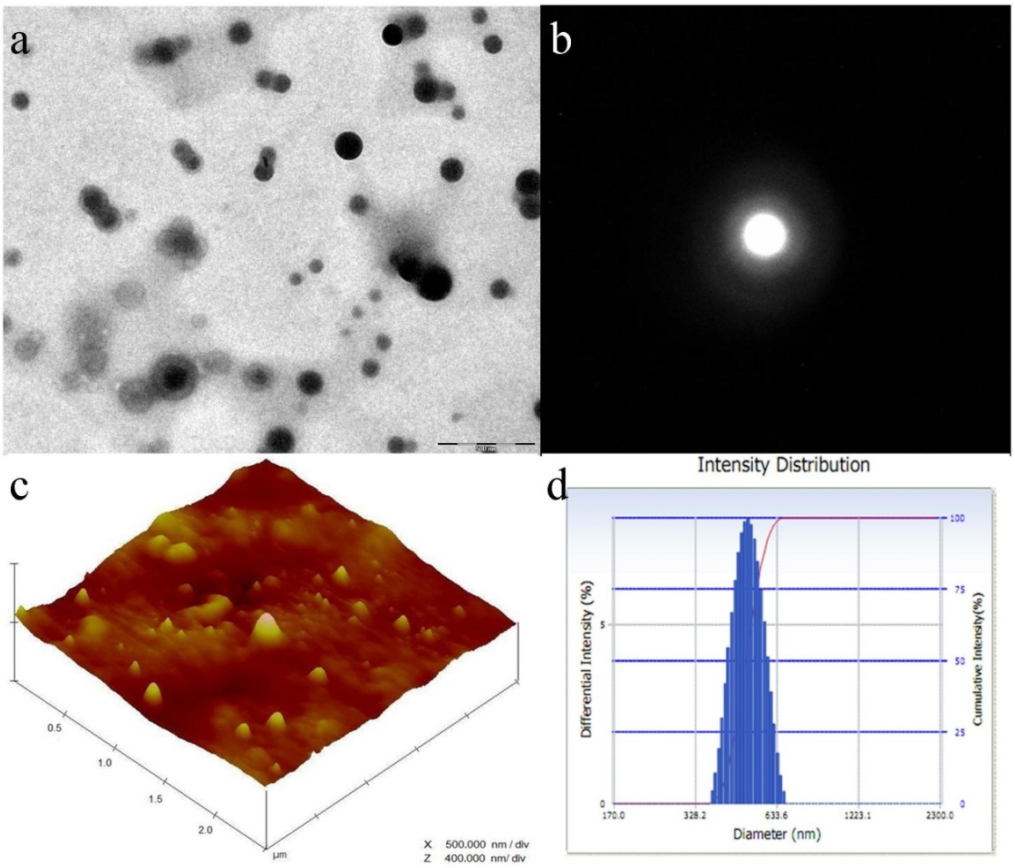

Fig. 4: (a) HR-TEM at 20 000× magnification (bar=500 µm); (b) Exhibits electron diffraction pattern of optimized Res-PNPs; (c) Surface morphology of optimized Res-PNPs measured by AFM (3D image) and (d) Mean PS of optimized Res-PNPs measured by PS analyzer (average diameter=410±9.78 nm, n=3)

The rate and extent of Res release might be directly related to the distribution coefficient of Res. Therefore, *in vitro* release data of Res from PNPs were fitted into several release kinetic equations such as zero order, first order, Higuchi, Hixon-crowel and Korsmeyer-Peppas model. The Higuchi equation was the best fit because of higher correlation coefficient (R^2=0.999) compared with other kinetic equations which having lower correlation coefficient as presented in Table 4. Further, revealed the release mechanism, Korsmeyer-Peppas model was the best fit with n value of 0.476 which indicated Fickian-diffusion mechanism of drug release from PNPs matrix (Table 4)[60,61].

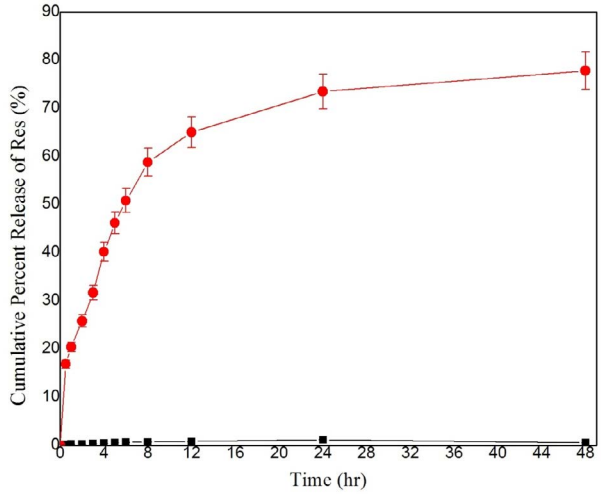

Fig. 5: *In vitro* release profile of pure Res and optimized Res-PNPs in PBS, pH 7.4 for 48 h (vertical bars represent mean±SD, n=3), (■) Free Res; (●) Optimized Res-PNPs

The optimized Res-PNPs were stable at room temperature for 9 mo and accelerated condition for 6 mo for all *in vitro* physicochemical parameters. There are no significant changes observed throughout the stability periods which indicated that the optimized Res-PNPs were highly stable as depicted in fig. 6a and fig. 6b, respectively.

Fig. 7 illustrated the plasma concentration-time curve obtained after oral administration of pure Res suspension, PM and optimized Res-PNPs. The Area under the Curve $(AUC)_{0-24}$ and Maximum Plasma Concentration (C_{max}) were found to be 1.98-fold, 1.57-fold as well as 4.07-fold, 5.03-fold greater when Res

TABLE 4: RELEASE PARAMETERS FOR OPTIMIZED RES-PNPs (BATCH RES-ENP3) OBTAINED AFTER FITTING *IN VITRO* RELEASE DATA TO FIVE DIFFERENT KINETIC MODELS

Batch	Zero order	First order	Higuchi model	Hixon-Crowel model	Korsemeyer-Peppas model
Res-ENP3	K_z=1.987 (Concentration/time) R^2=0.735	K_F=0.112 ($time^{-1}$) R^2=0.705	K_H=19.53 R^2=0.999	K_{HC}=0.101 R^2=0.899	K_p=0.367 R^2=0.977 n=0.476

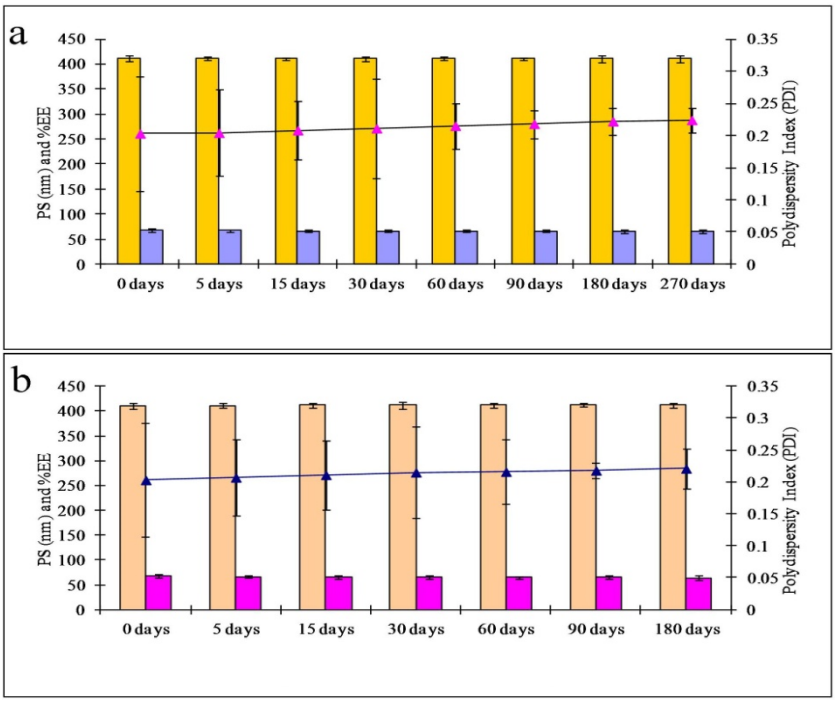

Fig. 6: Stability study data of the optimized Res-PNPs during storage, (a) At room temperature (25±2°/60 %±5 % RH) for 9 mo, (▬) PS (nm); (▬) % EE; (▲) PDI; (b) At accelerated condition (40±2°/75 %±5 % RH) for 6 mo (all data were performed in triplicate and the vertical bars represent mean±SD, n=3) (▬) PS (nm); (▬) % EE; (▲) PDI

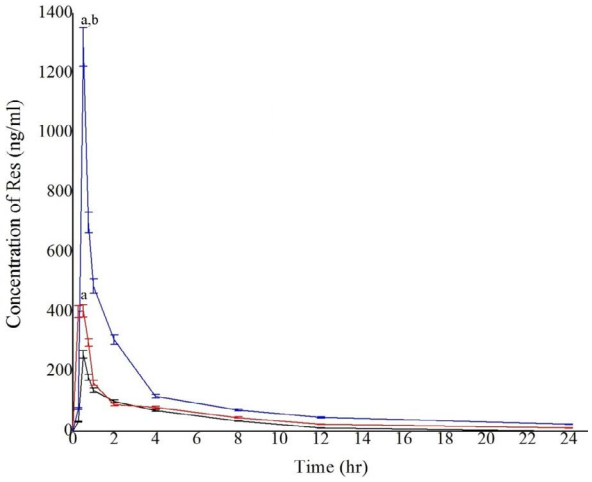

Fig. 7: Plasma concentration-time profile after oral administration of pure Res, PM and optimized Res-PNPs (dose 25 mg/kg in each group) vertical bars represent mean±SEM; n=6, [a]p<0.05, compared to the control (pure Res), [b]p<0.05, compared to PM, (One-way ANOVA; Tukey's multiple comparison test), (——) free Res; (——) PM; (——) Optimized ReS-PNPs

was administered as PM and optimized Res-PNPs, respectively when compared with pure Res aqueous suspension. It was observed that plasma levels declined stridently after 2 h which indicated that rapid systemic elimination and also proved by the short biological half-life of pure Res as presented in Table 5. These results thus recommended significantly ($p<0.05$) enhancement in oral bioavailability of Res in case of PM as well as optimized Res-PNPs; though, improvement of oral bioavailability of optimized Res-PNPs was significantly ($p<0.05$) higher than that of PM as well as pure Res.

The plasma level of Res after oral administration of pure Res was detected only up to 24 h with a C_{max} value of 256.004±12.80 ng/ml. The C_{max} and AUC_{0-24} of the drug were increased to 401.765±20.088 ng/ml and 1286.635±64.332 (ng/ml).h, respectively when PM was administered with the same dose. Further, the orally administered optimized Res-PNPs drastically enhanced the drug-plasma concentration (fig. 7). The AUC_{0-24} value of optimized Res-PNPs was significantly increased to 3056.458±128.248 (ng/ml).h (Table 5). The above results recommended that PM and optimized Res-PNPs significantly increased the oral bioavailability of Res; though, the enhancement of bioavailability with optimized Res-PNPs was significantly ($p<0.05$) higher compared with PM. Therefore, M-cells are thought to be comparatively less protected by mucus secretions and drug efflux transporters like P-glycoprotein and are a common delivery for PNPs. However, PNPs adhere and become coated in mucus may have restricted access to M-cells. This mechanism might be due to small PS, increase surface area, reduced diffusion layer thickness, favorable ZP, shape and hydrophobic surface of PNPs play a crucial task in the uptake across the Gastrointestinal (GI) membrane and were found to significantly amend the absorption profile. Furthermore, the enhanced oral bioavailability of Res may also be attributed to amorphous nature of drug inside the PNPs matrices[62] i.e. the original crystalline structure of the drug was absent in the PNPs; supersaturated condition of Res in the intestinal lumen by the use of pH-dependent carrier[63], means they may slow down nucleation or crystal growth by adsorption on the crystal interface, thereby overcrowding crystal growth and the supersaturated solution will be obtained. The concentration increasing mechanism can significantly enhance Res bioavailability; the good adhesion and site-specific of Res-PNPs to gastrointestinal mucosa due to EE100 polymer[62]. Moreover, the reason for the enhancement of AUC after oral administration would be due to the sustained action of PNPs inside the blood circulation. Further, the cationic nature of polymer also imparts the mucoadhesive property in the gastrointestinal membrane and permits absorption of PNPs for a longer period and thereby, allows availability of the drug in the systemic circulation for a longer period. This phenomenon can be easily identified in the comparative results of the Mean Residence Time (MRT) of the different studied formulations (pure Res, PM and optimized Res-PNPs). All of these phenomena might be the reason for the increased efficacy as compared to pure Res and PM. Furthermore, not only a small percentage of PNPs can be absorbed from the GI tract. Many types of research are in the area of oral bioavailability enhancement have claimed that a larger portion of the PNPs absorbed in the GIT and thereby, improve the oral bioavailability[64].

The PNPs containing Res were assessed to scavenge the $ABTS^+$ radical. The results of radical percentage inhibition gained from 1, 5, 10, 20 and 25 µM pure Res, PM and optimized Res-PNPs were examined at different time intervals 0, 24, 48 and 72 h as showed in Table 6.

At 0 h time point, it can be observed that the optimized Res-PNPs reveal the non-significant ($p>0.05$) similar scavenging activity of $ABTS^+$ at entire concentrations. The pure Res demonstrated a significantly ($p<0.05$) higher percentage of $ABTS^+$ inhibition compared with PM and optimized Res-PNPs. At the 24 h time point, both PM and optimized Res-PNPs exhibited similar inhibition as mentioned in the previous time point except optimized Res-PNPs exhibited significantly

TABLE 5: *IN VIVO* PHARMACOKINETIC DATA AFTER ORAL ADMINISTRATION OF PM AND OPTIMIZED RES-PNPs TO RATS, COMPARED WITH PURE RES AQUEOUS SUSPENSION (ALL VALUES REPORTED ARE MEAN±SEM; n=6)

Parameters	Pure Res (Control)	PM	Optimized Res-PNPs
C_{max} (ng/ml)	256.004±12.80	401.765±20.088	1286.635±64.332
T_{max} (h)	0.5±0.0	0.5±0.0	0.5±0.0
AUC_{0-24} (ng/ml). h	750.268±1.167	1488.965±48.378	3056.458±128.248
$AUMC_{0-24}$ (ng/ml). h^2	920.888±55.112	3417.395±174.219	22916.599±329.769
$t_{1/2}$ (h)	0.623±0.022	2.431±0.0752	5.598±0.198
MRT (h)	1.227±0.112	2.295±0.076	7.497±0.261

Note: C_{max}-Maximum plasma concentration; T_{max}-Time to reach maximum plasma concentration; AUC-Area under the plasma drug concentration-time curve; AUMC-Area under the first-moment plasma drug concentration-time curve; $t_{1/2}$-Half-life, MRT-Mean residence time

TABLE 6: PERCENTAGE INHIBITION OF RADICAL $ABTS^+$ OF PURE RES, PM AND OPTIMIZED RES-PNP_S AT DIFFERENT CONCENTRATIONS (1, 5, 10, 20 AND 25 µM) AND TIME POINTS (0, 24, 48 AND 72 h), RESPECTIVELY

Res concentration (µM)	Inhibition of $ABTS^{\cdot+}$ (%)		
	Pure Res	PM	Optimized Res-PNPs
0 h			
1	12.96±1.18[b]	5.86±1.01[a]	9.43±1.61[a]
5	44.25±2.43[b]	30.56±8.34[a,b]	16.52±0.43[a]
10	66.78±1.68[b]	36.87±6.86[a]	34.58±1.68[a]
20	93.57±3.89[b]	52.75±4.26[a]	57.89±2.66[a]
25	99.96±0.11[b]	66.01±6.91[a]	63.19±4.14[a]
24 h			
1	8.23±2.81[a]	4.95±0.94[a]	3.34±2.55[a]
5	29.27±3.57[b]	11.27±4.27[a]	15.25±2.08[a]
10	48.28±5.68[b]	21.67±1.68[a]	24.85±1.86[a]
20	95.75±6.98[b]	50.57±4.62[a]	55.88±3.67[a]
25	98.11±1.21[c]	66.69±4.19[a]	76.91±5.41[b]
48 h			
1	2.96±1.62[c]	2.68±0.92[a,c]	8.55±2.26[b]
5	24.52±3.28[a]	8.62±1.39[a]	22.92±2.43[a]
10	47.88±4.08[c]	19.82±1.55[a]	36.63±4.29[b]
20	89.28±5.19[c]	44.29±6.23[a]	63.57±5.69[b]
25	98.06±0.82[b]	68.38±5.49[a]	88.28±5.49[a,b]
72 h			
1	3.69±0.58[b]	11.68±1.91[a]	15.59±2.49[a]
5	29.56±3.22[b]	13.26±4.49[a]	26.89±1.43[b]
10	52.88±3.49[c]	25.78±3.19[a]	41.85±4.97[b]
20	92.75±4.11[c]	56.11±5.69[a]	71.99±6.81[b]
25	94.69±6.01[b]	76.22±4.33[a]	93.91±4.79[b]

Note: [a,b,c]Mean of triplicate±SD analyzed per line. Same letters mean statistical equality and inequality stats are indicated for different letters (ANOVA with Tukey's post-test and $p<0.05$)

($p<0.05$) and enhance $ABTS^+$ scavenging activity at a higher concentration, 25 µM. The pure Res significantly ($p<0.05$) decreased the $ABTS^+$ scavenging activity at three lower concentrations (1, 5 and 10 µM) but at higher concentrations (20 and 25 µM) insignificantly ($p>0.05$) same percentage radical inhibition as previous time point. At the 48 h time point, optimized Res-PNPs demonstrated significantly ($p<0.05$) increasing the radical inhibition, while PM exhibited the same profile at the 24 h time point. At higher concentration 25 µM, the optimized Res-PNPs exhibit insignificant ($p>0.05$) same activity but it was as effective as pure Res. At 72 h time point, optimized Res-PNPs demonstrated insignificant ($p>0.05$) similar scavenging activity as

TABLE 7: IC_{50} OF PURE RES, PM AND OPTIMIZED RES-PNP_S OVER THE CAPTURE OF $ABTS^+$ RADICAL IN SODIUM PHOSPHATE BUFFER (50 mM, pH 7.4) AND IN THE ABSENCE OF LIGHT AT ROOM TEMPERATURE (λ=734 nm)

Time (h)	IC_{50}		
	Pure Res±RSD*	PM±RSD*	Optimized Res-PNPs±RSD*
0	9.12±0.18[b]	16.68±0.81[a]	19.43±0.61[a]
24	11.35±0.23[c]	20.65±1.34[a]	17.25±0.88[b]
48	12.21±0.68[b]	20.87±1.76[a]	14.88±0.08[b]
72	11.89±0.89[b]	15.57±1.26[a]	13.22±0.61[b]

Note: [a,b,c]Mean of triplicate±SD analyzed per line. Same letters mean statistical equality and inequality stats are indicated for different letters (ANOVA with Tukey's post-test and $p<0.05$); RSD-Relative Standard Deviation

pure Res but the response gained from optimized Res-PNPs was significantly ($p<0.05$) inferior. In contrast, we can establish that two higher concentrations (20 and 25 μM) exhibited excellent scavenging activity for pure Res and optimized Res-PNPs. The scavenging activity profile with PM exhibited almost no enhancement in response at 24 h time point. Conclusively, the profile observed with optimized Res-PNPs demonstrated that excellent scavenging activity and increases with time[65-68].

The IC_{50} results of Res scavenging $ABTS^+$ as a function of time are presented in Table 7. The IC_{50} values of pure Res increase with time but optimized Res-PNPs demonstrated minor variations with time and show significant ($p<0.05$) superiority with pure Res. The IC_{50} values of optimized Res-PNPs decreased with time and after 48 and 72 h time points were considered insignificant ($p>0.05$) similar to pure Res.

In conclusion, the current investigation provides a profound insight into the attractive characteristics of oral Res-PNPs as an admirable hydrophobic antioxidant drug. The emulsification-diffusion-evaporation technique was effectively adopted for entrapment of Res molecules inside the PNPs and optimization was performed using the "Quality by design" approach. The Taguchi-orthogonal array design provided a high delta value followed by their rank and significant ($p<0.05$) ANOVA results. The optimization results recommended that physicochemical properties of Res-PNPs effectively been controlled by independent variables. The optimized PNPs demonstrated nanosized and monodispersed with no agglomeration between each other. The optimized Res-PNPs exhibited sympathetic mean PS, PDI, ZP, % EE, % DL and sustained release patterns followed by Fickian diffusion mechanism of drug release from PNPs matrix. The solid-state and morphological evaluation demonstrated the smooth and spherical architecture of PNPs, in which Res molecules were present in an amorphous form inside the PNPs matrix without any physical and chemical interactions. The optimized Res-PNPs were stable at room temperature and accelerated conditions. *In vivo* pharmacokinetics studies exposed that optimized Res-PNPs exhibited significantly ($p<0.05$) higher oral bioavailability as compared with pure Res suspension and PM. The optimized Res-PNPs were significantly ($p<0.05$) very effective as a scavenger of $ABTS^+$ radical which suggested that PNPs could be used for antioxidant molecules for the applications in prophylaxis or the treatment of several diseases including oxidative stress. Conclusively, the development of the PNPs approach can be an effective and safe vehicle for antioxidant, Res delivery in numerous therapies. The current research encourages and supports the feat of thorough preclinical studies with Res-encapsulated EE100 nanoparticles as a prerequisite for potentially advancing into human (clinical) applications.

PNPs embrace a clinical significance as a delivery stage for poorly soluble drugs and due to this reason, the recent formulation approach provides an efficient drug carrier. This carrier system can enhance the efficiency of translation from the lab to pre-clinical to clinical applications.

Acknowledgements:

The authors acknowledge Amity Institute of Pharmacy, Amity University, Noida, Uttar Pradesh, India for providing FT-IR facility and Mankind Research Centre, Unit-3, Gurgaon, India providing DSC and XRD facility.

Conflict of interests:

The authors declared no conflict of interest.

REFERENCES

1. Lucas-Abellán C, Mercader-Ros MT, Zafrilla MP, Gabaldón JA, Núñez-Delicado E. Comparative study of different methods to measure antioxidant activity of resveratrol in the presence of cyclodextrins. Food Chem Toxicol 2011;49(6):1255-60.
2. Finkel T, Holbrook NJ. Oxidants, oxidative stress and the biology of ageing. Nature 2000;408(6809):239-47.

3. Virgili F, Marino M. Regulation of cellular signals from nutritional molecules: A specific role for phytochemicals, beyond antioxidant activity. Free Radic Biol Med 2008;45(9):1205-16.
4. Schafer FQ, Buettner GR. Redox environment of the cell as viewed through the redox state of the glutathione disulfide/glutathione couple. Free Radic Biol Med 2001;30(11):1191-212.
5. Baur JA, Sinclair DA. Therapeutic potential of resveratrol: The *in vivo* evidence. Nat Rev Drug Discov 2006;5(6):493-506.
6. Gabaston J, Cantos-Villar E, Biais B, Waffo-Teguo P, Renouf E, Corio-Costet MF, *et al.* Stilbenes from *Vitis vinifera* L. waste: A sustainable tool for controlling *Plasmopara viticola*. J Agric Food Chem 2017;65(13):2711-8.
7. Adrian M, Jeandet P, Veneau J, Weston LA, Bessis R. Biological activity of resveratrol, a stilbenic compound from grapevines, against *Botrytis cinerea*, the causal agent for gray mold. J Chem Ecol 1997;23(7):1689-702.
8. Sobolev VS, Khan SI, Tabanca N, Wedge DE, Manly SP, Cutler SJ, *et al.* Biological activity of peanut (*Arachis hypogaea*) phytoalexins and selected natural and synthetic stilbenoids. J Agric Food Chem 2011;59(5):1673-82.
9. Kristl J, Teskač K, Caddeo C, Abramović Z, Šentjurc M. Improvements of cellular stress response on resveratrol in liposomes. Eur J Pharm Biopharm 2009;73(2):253-9.
10. Miura D, Miura Y, Yagasaki K. Hypolipidemic action of dietary resveratrol, a phytoalexin in grapes and red wine, in hepatoma-bearing rats. Life Sci 2003;73(11):1393-400.
11. Xia N, Daiber A, Förstermann U, Li H. Antioxidant effects of resveratrol in the cardiovascular system. Br J Pharmacol 2017;174(12):1633-46.
12. Jiang Z, Chen K, Cheng L, Yan B, Qian W, Cao J, *et al.* Resveratrol and cancer treatment: Updates. Ann NY Acad Sci 2017;1403(1):59-69.
13. Shi Y, Zhou J, Jiang B, Miao M. Resveratrol and inflammatory bowel disease. Ann N Y Acad Sci 2017;1403(1):38-47.
14. Hou CY, Tain YL, Yu HR, Huang LT. The effects of resveratrol in the treatment of metabolic syndrome. Int J Mol Sci 2019;20(3):535.
15. Cadena PG, Pereira MA, Cordeiro RB, Cavalcanti IM, Neto BB, Maria do Carmo CB, *et al.* Nanoencapsulation of quercetin and resveratrol into elastic liposomes. Biochim Biophys Acta Biomembr 2013;1828(2):309-16.
16. Amidon GL, Lennernäs H, Shah VP, Crison JR. A theoretical basis for a biopharmaceutic drug classification: The correlation of *in vitro* drug product dissolution and *in vivo* bioavailability. Pharm Res 1995;12(3):413-20.
17. Baur JA, Sinclair DA. Therapeutic potential of resveratrol: The *in vivo* evidence. Nat Rev Drug Discov 2006;5(6):493-506.
18. Walle T. Bioavailability of resveratrol. Ann N Y Acad Sci 2011;1215(1):9-15.
19. Walle T, Hsieh F, DeLegge MH, Oatis JE, Walle UK. High absorption but very low bioavailability of oral resveratrol in humans. Drug Metab Dispos 2004;32(12):1377-82.
20. Juan ME, Buenafuente J, Casals I, Planas JM. Plasmatic levels of trans-resveratrol in rats. Food Res Int 2002;35(2-3):195-9.
21. Amri A, Chaumeil JC, Sfar S, Charrueau C. Administration of resveratrol: What formulation solutions to bioavailability limitations? J Control Release 2012;158(2):182-93.
22. Jancova P, Anzenbacher P, Anzenbacherova E. Phase II drug metabolizing enzymes. Biomed Pap Med Fac Univ Palacky Olomouc Czech Repub 2010;154(2):103-6.
23. Wang P, Sang S. Metabolism and pharmacokinetics of resveratrol and pterostilbene. Biofactors 2018;44(1):16-25.
24. Ha ES, Choi DH, Baek IH, Park H, Kim MS. Enhanced oral bioavailability of resveratrol by using neutralized eudragit E solid dispersion prepared via spray drying. Antioxidants 2021;10(1):90.
25. Pignatello R, Pecora TM, Cutuli GG, Catalfo A, De Guidi G, Ruozi B, *et al.* Antioxidant activity and photostability assessment of trans-resveratrol acrylate microspheres. Pharm Dev Technol 2019;24(2):222-34.
26. Silva AF, Monteiro M, Resende D, Braga SS, Coimbra MA, Silva A, *et al.* Inclusion Complex of Resveratrol with γ-Cyclodextrin as a Functional Ingredient for Lemon Juices. Foods 2021;10(1):16.
27. Savić-Gajić I, Savić IM, Nikolić VD, Nikolić LB, Popsavin MM, Rakić SJ. The improvement of photostability and antioxidant activity of trans-resveratrol by cyclodextrins. Adv Tech 2017;6(2):18-25.
28. Parveen S, Misra R, Sahoo SK. Nanoparticles: A boon to drug delivery, therapeutics, diagnostics and imaging. Nanomedicine 2012;8(2):147-66.
29. Jung JY, Yoo SD, Lee SH, Kim KH, Yoon DS, Lee KH. Enhanced solubility and dissolution rate of itraconazole by a solid dispersion technique. Int J Pharm 1999;187(2):209-18.
30. Fessi HP, Puisieux F, Devissaguet JP, Ammoury N, Benita S. Nanocapsule formation by interfacial polymer deposition following solvent displacement. Int J Pharm 1989;55(1):R1-4.
31. Chaurasia S, Kumar N, Patel RR, Mishra B. Optimization of parameters for the fabrication of curcumin loaded polymeric nanoparticles using Taguchi robust design. Adv Sci Lett 2014;20(5-6):1028-38.
32. Waddad AY, Abbad S, Yu F, Munyendo WL, Wang J, Lv H, *et al.* Formulation, characterization and pharmacokinetics of Morin hydrate niosomes prepared from various non-ionic surfactants. Int J Pharm 2013;456(2):446-58.
33. D'Souza SS, DeLuca PP. Methods to assess *in vitro* drug release from injectable polymeric particulate systems. Pharm Res 2006;23(3):460-74.
34. Patel RR, Khan G, Chaurasia S, Kumar N, Mishra B. Rationally developed core–shell polymeric-lipid hybrid nanoparticles as a delivery vehicle for cromolyn sodium: Implications of lipid envelop on *in vitro* and *in vivo* behaviour of nanoparticles upon oral administration. RSC Adv 2015;5(93):76491-506.
35. Singh G, Pai RS, Pandit V. Development and validation of a HPLC method for the determination of trans-resveratrol in spiked human plasma. J Adv Pharm Technol Res 2012;3(2):130-5.
36. Wan L, Sun X, Li Y, Yu Q, Guo C, Wang X. A stereospecific HPLC method and its application in determination of pharmacokinetics profile of two enantiomers of naringenin in rats. J Chromatogr Sci 2011;49(4):316-20.
37. Buchanan CM, Buchanan NL, Edgar KJ, Little JL, Malcolm MO, Ruble KM, *et al.* Pharmacokinetics of tamoxifen after intravenous and oral dosing of tamoxifen–hydroxybutenyl-β-cyclodextrin formulations. J Pharm Sci 2007;96(3):644-60.
38. Re R, Pellegrini N, Proteggente A, Pannala A, Yang M, Rice-Evans C. Antioxidant activity applying an improved ABTS radical cation decolorization assay. Free Radic Biol Med 1999;26(9-10):1231-7.
39. Khalil OA, de Faria Oliveira OM, Vellosa JC, de Quadros AU, Dalposso LM, Karam TK, *et al.* Curcumin antifungal and antioxidant activities are increased in the presence of ascorbic acid. Food Chem 2012;133(3):1001-5.

40. Dillen K, Vandervoort J, Van den Mooter G, Ludwig A. Evaluation of ciprofloxacin-loaded Eudragit® RS100 or RL100/PLGA nanoparticles. Int J Pharm 2006;314(1):72-82.
41. Galindo-Rodriguez S, Allemann E, Fessi H, Doelker E. Physicochemical parameters associated with nanoparticle formation in the salting-out, emulsification-diffusion and nanoprecipitation methods. Pharm Res 2004;21(8):1428-39.
42. Uskokovic V. Entering the era of nanoscience: Time to be so small. J Biomed Nanotechnol 2013;9(9):1441-70.
43. Chakraborty S, Shukla D, Vuddanda PR, Mishra B, Singh S. Utilization of adsorption technique in the development of oral delivery system of lipid based nanoparticles. Colloids Surf B Biointerfaces 2010;81(2):563-9.
44. Mittal G, Sahana DK, Bhardwaj V, Kumar MR. Estradiol loaded PLGA nanoparticles for oral administration: effect of polymer molecular weight and copolymer composition on release behavior *in vitro* and *in vivo*. J Control Release 2007;119(1):77-85.
45. Sahana DK, Mittal G, Bhardwaj V, Kumar MR. PLGA nanoparticles for oral delivery of hydrophobic drugs: influence of organic solvent on nanoparticle formation and release behavior *in vitro* and *in vivo* using estradiol as a model drug. J Pharm Sci 2008;97(4):1530-42.
46. Govender T, Stolnik S, Garnett MC, Illum L, Davis SS. PLGA nanoparticles prepared by nanoprecipitation: drug loading and release studies of a water soluble drug. J Control Release 1999;57(2):171-85.
47. Govender T, Riley T, Ehtezazi T, Garnett MC, Stolnik S, Illum L, *et al.* Defining the drug incorporation properties of PLA–PEG nanoparticles. Int J Pharm 2000;199(1):95-110.
48. Panyam J, Williams D, Dash A, Leslie-Pelecky D, Labhasetwar V. Solid-state solubility influences encapsulation and release of hydrophobic drugs from PLGA/PLA nanoparticles. J Pharm Sci 2004;93(7):1804-14.
49. Chen Y, McCulloch RK, Gray BN. Synthesis of albumin-dextran sulfate microspheres possessing favourable loading and release characteristics for the anticancer drug doxorubicin. J Control Release 1994;31(1):49-54.
50. Chen Y, Mohanraj VJ, Parkin JE. Chitosan-dextran sulfate nanoparticles for delivery of an anti-angiogenesis peptide. Lett Pept Sci 2003;10(5-6):621-9.
51. Cui W, Li X, Zhou S, Weng J. Investigation on process parameters of electrospinning system through orthogonal experimental design. J Appl Polym Sci 2007;103(5):3105-12.
52. Bertacche V, Lorenzi N, Nava D, Pini E, Sinico C. Host-guest interaction study of resveratrol with natural and modified cyclodextrins. J Incl Phenom Macrocycl Chem 2006;55(3):279-87.
53. da Silva RD, Teixeira JA, Nunes WD, Zangaro GA, Pivatto M, Caires FJ, *et al.* Resveratrol: A thermoanalytical study. Food Chem 2017;237:561-5.
54. Kumar N, Chaurasia S, Patel RR, Kumar V, Mishra B. Development and optimization of atorvastatin calcium loaded oral biodegradable polymeric nanoparticles using central composite design. Adv Sci Lett 2014;20(5-6):984-93.
55. Zu Y, Zhang Y, Wang W, Zhao X, Han X, Wang K, *et al.* Preparation and *in vitro*/*in vivo* evaluation of resveratrol-loaded carboxymethyl chitosan nanoparticles. Drug Deliv 2016;23(3):971-81.
56. Kalita B, Das MK, Sarma M, Deka A. Sustained anti-inflammatory effect of Resveratrol-Phospholipid complex embedded polymeric patch. AAPS PharmSciTech 2017;18(3):629-45.
57. Muthu MS, Singh S. Studies on biodegradable polymeric nanoparticles of risperidone: *In vitro* and *in vivo* evaluation. Nanomed 2008;3(3):305-19.
58. Wong C, Yuen K, Peh K. Formulation and evaluation of controlled release Eudragit buccal patches. Int J Pharm 1999;178(1):11-22.
59. Bhagav P, Upadhyay H, Chandran S. Brimonidine tartrate–eudragit long-acting nanoparticles: formulation, optimization, *in vitro* and *in vivo* evaluation. AAPS PharmSciTech 2011;12(4):1087-101.
60. Costa P, Lobo JM. Modeling and comparison of dissolution profiles. Eur J Pharm Sci 2001;13(2):123-33.
61. Korsmeyer RW, Gurny R, Doelker E, Buri P, Peppas NA. Mechanisms of potassium chloride release from compressed, hydrophilic, polymeric matrices: effect of entrapped air. J Pharm Sci 1983;72(10):1189-91.
62. Wang XQ, Dai JD, Zhang H, Zhang X, Wang JC, Zhang Q. Absorption mechanism of cyclosporine A loaded pH-sensitive nanoparticles in rats. J Nanosci Nanotechnol 2008;8(5):2422-31.
63. Janssens S, De Zeure A, Paudel A, Van Humbeeck J, Rombaut P, Van den Mooter G. Influence of preparation methods on solid state supersaturation of amorphous solid dispersions: a case study with itraconazole and eudragit E100. Pharm Res 2010;27(5):775-85.
64. Jain AK, Swarnakar NK, Godugu C, Singh RP, Jain S. The effect of the oral administration of polymeric nanoparticles on the efficacy and toxicity of tamoxifen. Biomaterials 2011;32(2):503-15.
65. Lu X, Ji C, Xu H, Li X, Ding H, Ye M, *et al*. Resveratrol-loaded polymeric micelles protect cells from Aβ-induced oxidative stress. Int J Pharm 2009;375(1-2):89-96.
66. Re R, Pellegrini N, Proteggente A, Pannala A, Yang M, Rice-Evans C. Antioxidant activity applying an improved ABTS radical cation decolorization assay. Free Radic Biol Med 1999;26(9-10):1231-7.
67. da Rocha Lindner G, Khalil NM, Mainardes RM. Resveratrol-loaded polymeric nanoparticles: validation of an HPLC-PDA method to determine the drug entrapment and evaluation of its antioxidant activity. Sci World J 2013;2013.
68. Kim JH, Park EY, Ha HK, Jo CM, Lee WJ, Lee SS, *et al.* Resveratrol-loaded nanoparticles induce antioxidant activity against oxidative stress. Asian-Australas J Anim Sci 2016;29(2):288-98.